Research Square

Preprints are preliminary reports that have not undergone peer review.
They should not be considered conclusive, used to inform clinical practice,
or referenced by the media as validated information.

BAIAP2L2 is activated by NFκB1 and promotes the malignancy of hepatocellular carcinoma by suppressing the ubiquitin-mediated degradation of GABPB1 to activate TRET transcription

Wenbo Jia
The First Affiliated Hospital of Nanjing Medical University
Liang Yu
the Second Hospital of Anhui Medical University
Bin Xu
The First Affiliated Hospital of Nanjing Medical University
Yanzhi Feng
The First Affiliated Hospital of Nanjing Medical University
Jinyi Wang
The First Affiliated Hospital of Nanjing Medical University
Jian Chu
The First Affiliated Hospital of Nanjing Medical University
Deming Zhu
Chao Xu
The First Affiliated Hospital of Nanjing Medical University
Yongping Zhou
Wuxi Second Hospital, Nanjing Medical University
Lianbao Kong
Liver Transplantation Center, The First Affiliated Hospital of Nanjing Medical University
https://orcid.org/0000-0003-2508-1321
WenZhou Ding (✉ dingwenzhou@njmu.edu.cn)
The First Affiliated Hospital of Nanjing Medical University

Article

Keywords: BAIAP2L2, Hepatocarcinogenesis, GABPB1, Ubiquitination, TERT

Posted Date: August 29th, 2022

DOI: https://doi.org/10.21203/rs.3.rs-1945634/v1

License: This work is licensed under a Creative Commons Attribution 4.0 International License.
Read Full License

Abstract

Hepatocellular carcinoma (HCC) is one of the most commonly diagnosed human cancers in the world and the fourth leading cause of cancer-related death. In this study, we found that BAI1-associated protein 2-like 2 (BAIAP2L2) was upregulated in HCC tissues and was an independent risk factor for overall survival in HCC patients. BAIAP2L2 promoted cell proliferation, stem cell activity, and cell cycle progression and inhibited apoptosis in HCC. In addition, BAIAP2L2 enhanced HCC metastasis and activated the EMT pathway. At the molecular level, NFκB1 stimulated BAIAP2L2 transcription by binding directly to its promoter region. BAIAP2L2 interacted with GABPB1 to inhibit its ubiquitin-mediated degradation and promote its nuclear translocation. Moreover, BAIAP2L2 regulated telomerase reverse transcriptase (TERT) by upregulating GABPB1 and subsequently promoted cancer properties in HCC. Collectively, our study reveals the function and mechanism of BAIAP2L2 in HCC and provides a potential biomarker and therapeutic target for HCC.

Introduction

Hepatocellular carcinoma (HCC) is the main histological subtype of primary liver cancer, accounting for 80% of cases worldwide[1]. In global cancer statistics, the new incidence of liver cancer ranks seventh, and the mortality rate ranks second[2,3]. Surgical resection or transplantation is the most effective treatment for early-stage HCC. However, most patients with HCC do not have symptoms early on and are diagnosed at an advanced stage[4]. Although the prevention of, diagnosis of, and intervention for HCC have been improved, outcomes remain unfavorable. Therefore, it is important to improve the study of the molecular mechanisms underlying HCC pathogenesis.

BAI1-associated protein 2-like 2 (BAIAP2L2) belongs to the I-BAR protein family and has been reported to play a key role in many cancers, including lung cancer[5], osteosarcoma[6], gastric cancer[7] and prostate cancer[8]. In gastric cancer, BAIAP2L2 promotes cancer progression via the AKT/mTOR and Wnt3a/beta-catenin signaling pathways[7]. BAIAP2L2 inhibition restrained the proliferation of osteosarcoma cells[6]. Furthermore, BAIAP2L2 is a potential therapeutic target for EGFR wild-type cancers with low PD-L1 expression[9]. Nevertheless, the clinicopathological importance of BAIAP2L2 in HCC is unknown, and no study has been performed to clarify the functional role of BAIAP2L2 during HCC development.

In this study, we revealed that BAIAP2L2 was upregulated in HCC and was an independent risk factor for the overall survival of HCC patients. BAIAP2L2 could promote HCC cell proliferation, stem cell activity, and cell cycle progression and inhibit apoptosis. In addition, BAIAP2L2 enhanced HCC cell invasion and migration and activated the EMT pathway. In vivo experiments also confirmed that BAIAP2L2 promoted HCC proliferation and metastasis. The upregulation of NF-κB1 played a central role in mediating BAIAP2L2 upregulation in HCC. We further illustrated that BAIAP2L2 interacted with GABPB1. BAIAP2L2 inhibited protease degradation of GABPB1 by inhibiting its ubiquitination and promoting its nuclear translocation. Moreover, BAIAP2L2 regulated TERT by upregulating GABPB1 and subsequently promoting

cancer development in HCC. The results of our analysis indicated that BAIAP2L2 may be a diagnostic biomarker and a therapeutic target for HCC.

Materials And Methods

Cell lines and human tissue

HCC cells (Huh7, MHCC97 L, HepG2, Hep3B, MHCCLM3, Focus and YY8103), immortalized human hepatocyte THL1-3 cells and HEK293T cells were obtained from the Shanghai Institute of Cell Biology, Chinese Academy of Sciences (Shanghai, China).

HCC tissues and paracancerous samples were acquired from patients undergoing hepatic resection at the Hepatobiliary Centre of the First Affiliated Hospital of Nanjing Medical University. All participants in this study provided written informed consent approved by the Ethics Committee of the First Affiliated Hospital of Nanjing Medical University and conducted human experiments in accordance with the ethical norms of the World Medical Association (Declaration of Helsinki).

Cell culture and transfection

All cells were cultured in Dulbecco's modified Eagle's medium (DMEM) (Invitrogen, Carlsbad, USA) supplemented with 10% fetal bovine serum (Gibco, Carlsbad, USA) and 50 U/ml penicillin—streptomycin (Invitrogen). The cells were cultured in a 5% CO2 incubator at 37 °C. Lentiviruses overexpressing BAIAP2L2, lentivirus-embedded BAIAP2L2 small hairpin RNA (shRNA), NFκB1 small interfering RNA, NFκB1 overexpression plasmid, GABPB1 small interfering RNA and GABPB1 overexpression plasmid were obtained from GenePharma (GenePharma, Shanghai, China). The shRNA and siRNA sequences are provided in Supporting Table 2.

Quantitative real-time PCR (qRT—PCR)

Total RNA of HCC tissues and HCC cell lines was isolated with an RNA extraction kit (Invitrogen). Then, the total RNA was transcribed to cDNA with a Prime Script RT kit (TaKaRa, Dalian, China). Quantitative real-time PCR was performed with SYBR Premix ExTaq II (TaKaRa). The results were calculated according to the $2^{-\Delta\Delta CT}$ method[10] and the primer sequences are shown in Supporting Table 1.

Cell counting kit-8 (CCK-8) analysis

Transfected cells were plated in a 96-well plate. CCK-8 solution (RiboBio, Guangzhou, China) was added every 24 hours (h) according to the manufacturer's protocol. Continuous testing was performed for 5 days.

Wound healing assay

Wound healing assay was performed to detect the capacities of cell migration. In brief, the transfected cells were plated in 6-well plates and the surface of the cells were scratched with a 200 μl plastic pipette tip. Wound closure was monitored at 0 h and 48 h.

Transwell assay

In the cell migration experiment, 2×10^4 cells were seeded in the upper chamber of a transwell chamber (Corning, NY, USA) with 200 μL of serum-free DMEM. Then, 600 μL of DMEM containing 10% FBS was added to the lower chamber. For the cell invasion experiment, Matrigel (diluted 1:8; BD Biosciences, Franklin Lakes, USA) was added to the upper chamber, and the other steps were the same as those in the migration experiment. Incubation occurred for 48 hours. The upper cells were removed and cells were fixed and stained for quantitative analysis.

5-Ethynyl-20-deoxyuridine (EdU) assay

Transfected cells were incubated with EdU solution (RiboBio) in 24-well plates for 2 h. Then, cells were fixed and aldehyde groups were neutralized with 2 mg/ml glycine. Cells were permeated with 0.5% Triton X-100 and then stained with Apollo and DAPI.

Sphere-forming assay

Stem cell culture medium: DMEM/F12 (Gibco) supplemented with 1X B27 (Sigma–Aldrich, Saint Louis, USA), 20 ng/mL EGF (PeproTech, NJ, USA), 20 ng/mL FGF (PeproTech) and 4 μg/ml heparin. A total of 2000 cells in 2 mL of stem cell culture medium were seeded in a 24-well suspension cell culture plate (Corning) for 10 days. The pellet-forming status of the cells was observed, and the size and number of pellets were calculated.

Construction of hepatocellular carcinoma organoid model

The organoid culture protocol followed a previous method[11].

The patient-derived specimens were minced and incubated with the digestive solution for 4 h at 37 °C. Cells were then mixed with BME (R&D Systems) on ice. A total of 2000 cells were seeded per well in an ultralow adsorption 24-well plate and were cultured in the advanced DMEM/F12 (Gibco) supplemented with 1% penicillin/streptomycin, 1% Glamax, 10 mM HEPES, 1:50 B27 supplement (Sigma–Aldrich), 1:10 N2 supplement (Sigma–Aldrich), 1.5 mM N-acetyl-l-cysteine (Sigma–Aldrich), 20% (vol/vol) Rspo-1 conditioned medium (Univ, Shanghai, China), 20% (vol/vol) Wnt3a conditioned medium (Univ), 15 mM nicotinamide (Sigma–Aldrich), 15 nM recombinant human gastrin I (Sigma–Aldrich), 40 ng/ml recombinant human EGF (PeproTech), 100 ng/ml recombinant human FGF10 (PeproTech), 20 ng/ml recombinant human HGF (PeproTech), 15 μM forskolin (R&D Systems, MND, USA), 10 μM A8301 (R&D Systems), 20 ng/ml Noggin (Univ), and 15 μM Y27632 (Sigma–Aldrich).The medium was changed twice a week.

Western blot assay

Cells were lysed with radioimmunoprecipitation (RIPA) buffer prechilled with the addition of 1 mM phenylmethylsulfonyl fluoride (PMSF). After adding loading buffer and boiling for 10 min to denature the protein, proteins were separated using sodium dodecyl sulfate–polyacrylamide gel electrophoresis (SDS–PAGE) and then transferred to polyvinylidene fluoride (PVDF) membranes (Bio-Rad, CA, USA). The proteins were incubated with primary antibodies overnight at 4 °C and secondary antibodies for 2 h at room temperature and visualized by ECL (Yesen, Shanghai, China) detection. The antibodies are shown in Supporting Table 2.

Flow cytometry analysis

In the cell cycle analysis, after the cells were fixed, 5×10^5 cells were added to each tube and stained with propidium iodide (PI) (Vazyme, Nanjing, China). Cell cycle distribution was measured by a BD FACS Canto II. In the cell apoptosis analysis, transfected cells were stained by Annexin V-FITC solution (Vazyme) and PI solution according to the manufacturer's instruction and apoptosis was detected via BD FACS Canto II.

Luciferase reporter assay

The BAIAP2L2 promoter sequence was obtained from the UCSC database (http://genome. ucsc.edu/) and the BAIAP2L2 promoter regions (−2000/0, −1500/0, −1000/0, −750/0, −500/0 and −250/0) were inserted into the pGL3-Basic vector (Promega, Madison, USA) to construct a luciferase reporter gene. Two single-site mutation (-522 ~ -532) mut and (-984 ~ -994 bp) mut and two-site mutation (-522 ~ -532 mut and -984 ~ -994 bp) sequences of BAIAP2L2 promoter were inserted into the pGL3-Basic vector. The relevant plasmids were transfected into 293T cells using Lipofectamine 3000 (Invitrogen). Dual-luciferase reporter gene assays were conducted with the Dual-Luciferase Reporter Assay System (Promega).

Animal models

All animal experiments were performed in accordance with National Institutes of Health guidelines and authorized by the local ethics committee of the First Affiliated Hospital of Nanjing Medical University. Four-week-old male BALB/c nude mice were purchased from the Model Animal Research Centre of Nanjing Medical University (Nanjing, China). The transfected cells were injected into the flanks of nude mice and tumor size was recorded every 3 days for 4 weeks. The volumes of the tumors were calculated by the formula: $\text{length} \times \text{width}^2/2$.

For the orthotopic tumor transplantation model, the required cells were prepared into a 5×10^7/mL cell suspension. After successful isoflurane anesthesia, the nude mice were disinfected under the xiphoid process of the midabdominal line, and an approximately 0.5 cm incision was made to expose the left lobe of the liver. A total of 20 μl of cell suspension was injected under the liver capsule. At week 4, the

fluorescence distribution and intensity of the abdominal liver were observed, and then the nude mice were sacrificed for liver analysis.

The lung metastasis model was established by tail vein injection. There were 15 nude mice in each group, and each mouse was injected with approximately 1×10^6 posttransfected cells through the tail vein. At week 4, 5 mice per group were sacrificed. Survival analysis was performed on the remaining mice with a 12-week cutoff.

Chromatin immunoprecipitation assays

A ChIP Assay Kit (Beyotime, Shanghai, China) was used to perform chromatin immunoprecipitation (ChIP) assays. Briefly, after cell lysis, the chromatin was lysed to 200-2000 bp through an ultrasonic cytometer and immunoprecipitated with NFκB1 and IgG controls. The enriched DNA templates were analyzed by qRT–PCR analysis using primer pairs for each target gene promoter (Supporting Table 1).

Coimmunoprecipitation (Co-IP) assay

The interactions between BAIAP2L2 and GABPB1 and GABPB1 and ubiquitin were detected by the Co-IP method. BAIAP2L2 or GABPB1 antibodies were incubated with protein lysate overnight, and the complexes were precipitated using protein A/G-agarose beads (Beyotime). Immunoprecipitated products were analyzed by western blot.

Immunofluorescence assay and confocal microscopy

Cells cultured on confocal dishes were fixed and permeabilized 10 min. The rabbit antibody BAIAP2L2 and mouse antibody GABPB1 were added and incubated overnight. Then, cells were stained with Alexa Fluor 594 goat anti-rabbit IgG and Alexa Fluor 488 goat anti-mouse IgG. Nuclei were labeled with DAPI, and cells were visualized with a confocal laser scanning microscope (Olympus).

Immunohistochemistry (IHC)

The IHC and the tissue microarray assay were performed as described previously[28]

RNA sequencing

Three pairs of HCC specimens were lysed with TRIzol reagent. Next, RNA sequencing (JI GUANG Gene, Nanjing, China) was performed. RNA-sequencing data are presented in Supplementary Table 2.

Statistical analysis

SPSS version 22.0 (Chicago, IL, USA) and GraphPad Prism version 7.0 software (La Jolla, CA, USA) were used for statistical analysis. Student's t test was used to analysis the differences between two groups. Quantitative data were recorded as the mean ± standard deviation. Kaplan–Meier estimates were used to

plot survival rates, and cox proportional hazards regression analysis was used to analyze the independent factors for prognosis. Statistical significance was defined as $p < 0.05$ (*), $p < 0.01$ (**), and $p < 0.001$ (***).

Results

The expression of BAIAP2L2 was upregulated in HCC and correlated with poor outcome.

To explore HCC-related genes, we examined three pairs of HCC tumor and paracancerous tissues by high-throughput sequencing. The results showed that BAIAP2L2 was highly expressed in HCC tissues (fold change: 11.83) (Fig. 1A, Supplementary Table 1). Pan-cancer analysis in TCGA database revealed that BAIAP2L2 expression was upregulated in HCC tissues compared with normal tissues (Fig. S1A). To further investigate the expression of BAIAP2L2, 80 pairs of HCC tumor and paracancerous tissues were measured by qRT—PCR. The results revealed that BAIAP2L2 mRNA was upregulated in HCC tissues (Fig. 1B, C). Western blot (Fig. 1D) and immunohistochemistry (IHC) (Fig. 1E, 1F, Fig. S1B) further confirmed that the BAIAP2L2 protein was also upregulated in HCC tissues. Furthermore, BAIAP2L2 mRNA and protein in HCC cell lines and the human hepatocyte cell line THL1-3 were measured by qRT—PCR and western blot. The results showed that both BAIAP2L2 mRNA and protein were upregulated in all seven HCC cell lines compared with THL1-3 (Fig. S2A, B). The clinicopathological analysis showed that BAIAP2L2 expression was closely related to tumor multiplicity, tumor size, Edmonson stage, vascular invasion and tumor-node-metastasis (TNM) stage (Table 1). Patients with high BAIAP2L2 expression had poorer overall survival. (Fig. 1G). Additionally, the data from GEPIA also showed that the expression of BAIAP2L2 is negatively correlated with overall survival and disease-free survival of HCC patients (Fig. S2C, D). Univariable (Fig. S2E, $P < 0.001$) and multivariable (Fig. 1H, $P = 0.024$) analyses demonstrated that BAIAP2L2 was an independent factor for the overall survival of HCC individuals (Table 2). These results indicate that BAIAP2L2 may play an important role in the progression of HCC and possibly serve as a prognostic marker.

BAIAP2L2 promoted cell proliferation and stem cell activity in HCC.

According to the expression level of BAIAP2L2 in HCC cell lines (Fig. S2A, B), we used lentivirus to stably overexpress BAIAP2L2 in Hep3B and YY8103 cells, which exhibited lower BAIAP2L2 expression than the others. BAIAP2L2 was knocked down by lentivirus carrying small hairpin RNA (shRNA) in HCCLM3 and Focus cells with high BAIAP2L2 expression. The knockdown and overexpression efficiency for BAIAP2L2 was detected by western blot (Fig. 2A, B). Of the three shRNAs tested, shBAIAP2L2-3 produced the most consistent knockdown results in HCCLM3 and Focus cell lines; therefore, shBAIAP2L2-3 was selected and used in subsequent experiments. To evaluate the effect of BAIAP2L2 on HCC cell proliferation, we performed CCK-8, colony formation and EdU experiments. The above experiments all showed that downregulation of BAIAP2L2 significantly inhibited proliferation in HCCLM3 and Focus cells (Fig. 2C, E, G), while BAIAP2L2 overexpression promoted the proliferation of Hep3B and YY8103 cells (Fig. 2D, F, H).

HCC is heterogeneous and contains cells with stem-like properties[12,13]. Cancer stem cells (CSCs) are believed to be involved in the initiation and progression of HCC[14,15]. We used sphere-forming assays to separate CSCs from HCC cell lines. The results showed that spherical structures were attenuated in BAIAP2L2-knockdown HCCLM3 and Focus cells and promoted in BAIAP2L2-overexpressing Hep3B and YY8103 cells (Fig. 2I). Meanwhile, the expression of CSC-associated markers (CD133, CD44, CD24, CD90, EpCAM) was measured by qRT—PCR assay. The results suggest that BAIAP2L2 knockdown downregulates the expression of stemness-related transcription factors and CSC-related biomarkers. Overexpression of BAIAP2L2 had the opposite effect (Fig. 2J). To further validate our findings, three-dimensional organoids derived from HCC patients were created. We stably altered the expression of BAIAP2L2 by lentivirus carrying shRNA or an overexpression plasmid and analyzed the expression of BAIAP2L2 in HCC tissue organoids using qRT–PCR (Fig. 2L). The results indicated that BAIAP2L2 knockdown resulted in smaller tumor organoids, whereas BAIAP2L2-overexpressing cells formed larger spheres (Fig. 2K, M).

BAIAP2L2 promoted cell migration and invasion and activated the EMT pathway in HCC.

We investigated the role of BAIAP2L2 in HCC cell migration and invasion via wound healing and transwell assays. Both assays showed that downregulation of BAIAP2L2 suppressed cell migration and invasion in HCCLM3 and focus cells, while overexpression of BAIAP2L2 strengthened the migration and invasion capacities of Hep3B and YY8103 cells (Fig. 3A-D).

Studies have shown that the migration and invasion ability of tumor cells are closely related to the epithelial-mesenchymal transition (EMT) process[16]. Immunofluorescence results showed that BAIAP2L2 knockdown inhibited the expression of N-cadherin and vimentin and promoted the expression of E-cadherin. BAIAP2L2 overexpression had the opposite effect (Fig. 3E). These results indicated that BAIAP2L2 activated the EMT process, thus promoting the migration and invasion capacities of HCC cells.

BAIAP2L2 induced the G1/S cell cycle and inhibited apoptosis in vitro.

To investigate the potential role of BAIAP2L2 in HCC cell apoptosis, flow cytometry and western blot analyses were performed. As shown in Fig. 4A, upregulated BAIAP2L2 suppressed cell apoptosis, while downregulated BAIAP2L2 promoted cell apoptosis. We further detected apoptosis-related factors by western blotting. BAIAP2L2 overexpression inhibited the expression of cleaved Caspase 3 and cleaved Caspase 9 but increased Bcl2 expression. BAIAP2L2 knockdown had the opposite effect. (Fig. 4B).

By quantitatively analyzing the cell cycle distribution through flow cytometry, we found that overexpression of BAIAP2L2 increased the number of cells in the S and G2 phases of Hep3B cells, and downregulation of BAIAP2L2 decreased the number of HCCLM3 cells in the S and G2 phases. Furthermore, we detected the expression of cyclin-dependent kinase 6 (CDK6) and cyclin-dependent kinase 4 (CDK4) by western blotting. The results showed that overexpression of BAIAP2L2 promoted the expression of CDK4 and CDK6, and knockdown of BAIAP2L2 had the opposite result (Fig. 4D). The above

experiments demonstrated that BAIAP2L2 suppressed cell apoptosis and enhanced cell cycle progression in HCC.

BAIAP2L2 facilitated tumor growth and metastasis in vivo.

To further investigate the role of BAIAP2L2 in cell proliferation, we established a subcutaneous tumor model and orthotopic xenograft model. For the subcutaneous tumor model, the results suggested that BAIAP2L2 silencing attenuated tumor growth, while BAIAP2L2 overexpression promoted tumor growth, as reflected in tumor volume and weight (Fig. 5A-C). IHC of subcutaneous tumors indicated that BAIAP2L2 overexpression in YY8103 cells increased Ki67 and vimentin expression while decreasing E-cadherin and TUNEL staining, whereas the opposite effects were observed in HCCLM3 cells with BAIAP2L2 downregulation (Fig. 5D). The biological effect of BAIAP2L2 was further elucidated in vivo in an orthotopic xenograft model. The experiment also suggested that BAIAP2L2 knockdown inhibited, while overexpression of BAIAP2L2 promoted, the growth of HCC cells in nude mouse liver (Fig. 5E-G). These data illustrated that BAIAP2L2 stimulates HCC cell growth and EMT and inhibits apoptosis in vivo.

To explore the effect of BAIAP2L2 on HCC cell metastasis in vivo, we constructed a nude mouse lung metastasis model. Bioluminescence imaging and lung HE staining showed that BAIAP2L2 knockdown significantly inhibited lung metastasis and that BAIAP2L2 overexpression resulted in increased lung metastasis nodules (Fig. 5H-K). In addition, E-cadherin and vimentin staining of lung metastases demonstrated that BAIAP2L2 promoted EMT signaling pathway activity in vivo (Fig. 5J). The mouse survival analysis of this model showed that the overall survival time of the mice in the overexpression group was significantly reduced, while the opposite results were observed in the knockdown group (Fig. 5L). Taken together, these results further demonstrated that BAIAP2L2 promoted HCC cell proliferation and metastasis.

NFκB1 activated BAIAP2L2 transcription in HCC cells.

We explored the potential regulators involved in the upregulation of BAIAP2L2 by analyzing the promoter of BAIAP2L2. As shown in Fig. 6A and B, BAIAP2L2 promoter activity decreased significantly in the −1000 to -500 region, suggesting that the − 1000/−500 region was required for the transcription of BAIAP2L2. To identify transcription factors of BAIAP2L2 in HCC cells, we used the online software PROMO program to predict transcription factors and their binding sites in the − 1000/−500 region. Meanwhile, we obtained the top transcription factor-binding sites by QIAGEN in the BAIAP2L2 gene promoter. NFκB1 and PAX-5 were predicted to be transcription factors of BAIAP2L2 by the two databases (Fig. 6C). Then, NFκB1 and PAX-5 were overexpressed in 293T cells transfected with pGL3-1000 respectively. pGL3-1000 promoter activity was significantly enhanced in the NFκB1 overexpression group but not in the PAX-5 overexpression group (Fig. 6D). We knocked down the expression of NFκB1 in HCCLM3 cells with siRNA and upregulated the expression of NFκB1 in Hep3B cells with plasmids. Western blot results showed that BAIAP2L2 expression was downregulated in NFκB1-knockdown HCCLM3 cells and upregulated in NFκB1-overexpressing Hep3B cells (Fig. 6E). Spearman correlation analysis revealed that BAIAP2L2 expression was positively correlated with NFκB1 levels in 80 pairs of

HCC tissues (Fig. 6F). Next, we determined whether NFκB1 could bind to the promoter of BAIAP2L2 by ChIP assay. As shown in Fig. 6G, in HCCLM3 and Hep3B cells, the BAIAP2L2 promoter was enriched by the anti-NFκB1 antibody. We further obtained the NFκB1 binding motif from the JASPAR database (Fig. 7H) and obtained two NFκB1-binding sites with high scores in the promoter of BAIAP2L2 by PROMO. To explore the role of the two putative NFκB1 binding sites in the regulation of the BAIAP2L2 promoter, we designed three mutations: (− 522 to − 532 bp) mut, (− 984 to − 994 bp) mut and two-site mutation sites (− 522 to − 532 bp, − 984 to − 994 bp) mut (Fig. S3A). The results of the luciferase reporter assay showed that in HCCLM3 and Hep3B cells, the promoter activity of single-site mutant plasmids (− 522 ~ − 532 bp, − 984 ~ − 994 bp) decreased by 40% ~ 60% compared with wild-type controls, respectively. The double site mutant plasmid promoter activity was reduced by 80–90% (Fig. 6I). These data suggested that the two NFκB1 binding sites function independently. Taken together, NFκB1 stimulated BAIAP2L2 transcription in HCC by binding directly to its promoter region.

BAIAP2L2 inhibited the ubiquitin-mediated degradation of GABPB1 and promoted GABPB1 nuclear translocation.

To explore the mechanism of BAIAP2L2 in HCC, we used BioGRID, STRING and HitPredict to predict the proteins bound to BAIAP2L2. As shown in Fig. 7A, GAPBP1 and GRXCR1 were predicted to be putative BAIAP2L2-interacting proteins by all three databases. GABPB1 has been reported to be upregulated in various tumors, including HCC. Studies have shown that downregulation of GABPB1 in HCC results in rapid accumulation of ROS[17], which suggests that GAPPB1 affects HCC progression. Therefore, we focused on the ability of BAIAP2L2 to interact with GAPBP1 to promote HCC progression. Co-IP assays showed that GABPB1 was immunoprecipitated with anti-BAIAP2L2 antibody, and BAIAP2L2 could also be enriched by anti-GABPB1 antibody (Fig. 7B). Co-IP analysis using full-length and truncated BAIAP2L2 (Fig. S3B) indicated that the Src homology 3 (SH3) domain (331–385 aa) of BAIAP2L2 was primarily responsible for its interaction with GABPB1 (Fig. 7C, Fig. S3C). In addition, immunofluorescence (IF) results also showed that GABPB1 and BAIAP2L2 colocalized in Hep3B and HCCLM3 cells (Fig. 7D, Fig. S3D).

To further assess the effect of BAIAP2L2 binding on GABPB1, the protein stability of GABPB1 was detected with cycloheximide (CHX, a protein synthesis inhibitor), and the results showed that the degradation rate of GABPB1 was significantly slowed down when BAIAP2L2 was overexpressed and increased when BAIAP2L2 was knocked down (Fig. 7E, F). GABPB1 protein expression was decreased in BAIAP2L2 knockdown HCCLM3 cells and upregulated in BAIAP2L2-overexpressing Hep3B cells (Fig. 7G). In addition, the proteasome inhibitor MG132 restored the decrease in GABPB1 protein levels induced by BAIAP2L2 knockdown. (Fig. 7H). Furthermore, ubiquitination of GABPB1 was enhanced in BAIAP2L2-knockdown HCCLM3 cells and decreased in BAIAP2L2-overexpressing Hep3B cells (Fig. 7I). These results indicated that BAIAP2L2 inhibited the proteasomal degradation of GABPB1 by inhibiting its ubiquitination.

Interestingly, immunofluorescence (IF) results revealed that the nuclear translocation of GABPB1 was significantly increased in BAIAP2L2-overexpressing Hep3B cells (Fig. 7J). We then detected the protein level of GABPB1 in the nucleus and cytoplasm of HCC cells. The results showed that the expression of GABPB1 was markedly increased in the nucleus of BAIAP2L2-overexpressing Hep3B cells and was decreased in the nucleus of BAIAP2L2-knockdown HCCLM3 cells (Fig. 7K). These results demonstrated that BAIAP2L2 promoted the nuclear translocation of GABPB1.

BAIAP2L2 promoted HCC cell progression by interacting with GABPB1.

To explore the effect of BAIAP2L2 regulating GAPPB1 on HCC progression, we upregulated the expression of GABPB1 in HCCLM3-shBAIAP2L2 cells. The results demonstrated that the decreased ability of HCCLM3-shBAIAP2L2 cells to proliferate (Fig. S4A-C), form hepatospheres (Fig. S4D), migrate (Fig. S4E), progress through the cell cycle (Fig. S4H) and resist apoptosis (Fig. S4G) was reversed by GABPB1 overexpression. Meanwhile, we knocked down GABPB1 in Hep3B-BAIAP2L2 cells, and the results revealed that GABPB1 knockdown diminished the proliferation, migration, invasion, stem cell activity, cell cycle progression, and apoptosis of Hep3B-BAIAP2L2 cells (Fig. S5A-G).

BAIAP2L2 regulates TERT by upregulating GABPB1.

Studies have found that the GABPA-GABPB1 complex can bind and activate the mutated telomerase reverse transcriptase (TERT) promoter, significantly upregulating the expression of TERT[18,19] (Fig. 8A). TERT is a component of telomerase[20]. The induction and activation of TERT occurs frequently during tumor development and is closely related to tumor cell proliferation, invasion, and apoptosis[21, 22]. We thus hypothesized that BAIAP2L2 could regulate TERT by upregulating GABPB1 and subsequently promoting cancer properties in HCC. The qRT—PCR results showed that BAIAP2L2 silencing in HCCLM3 cells induced the downregulation of TERT, and GABPB1 upregulation rescued the downregulation of TERT induced by BAIAP2L2 silencing (Fig. 8B). This result was further confirmed by western blot (Fig. 8D). The opposite results were obtained in Hep3B cells with BAIAP2L2 overexpression and GABPB1 knockdown (Fig. 8C, E). In addition, Spearman correlation analysis showed that BAIAP2L2 expression was positively correlated with TERT (Fig. 8F). Collectively, these data suggest that BAIAP2L2 can upregulate TERT by interacting with GABPB1 in HCC cells.

Discussion

HCC is one of the most lethal malignancies in the world. Due to the lack of early diagnostic indicators of HCC, as well as its high proliferation and highly invasive characteristics, many patients have passed the time where surgery might be indicated by the time of diagnosis. With the emergence of targeted drugs such as sorafenib, lenvatinib and immunotherapy based on immune checkpoint inhibitors (ICPIs), the prognosis of HCC patients has been markedly transformed. However, many patients still cannot benefit from existing targeted drugs. Therefore, it is important to improve the mechanism of HCC development and to find sensitive therapeutic targets or prognostic biomarkers.

To explore the key genes involved in the progression of HCC, we obtained HCC-related gene profiles by high-throughput sequencing. BAIAP2L2 was significantly increased in HCC tissues. BAIAP2L2, also known as Pinkbar, is a member of the I-BAR protein family, located on chromosome 22q13.1[23] and was originally found to be involved in the regulation of cell membrane formation[24]. The I-BAR family plays a key role in the generation of membrane filopodia during cell migration and morphogenesis[25]. Previous studies have shown that BAIAP2L2 maintains a regulatory role in tumorigenesis. In prostate cancer, BAIAP2L2 was demonstrated to promote prostate cancer progression through VEGF and apoptosis signaling pathways[26]. Guo et al. demonstrated that BAIAP2L2 promotes osteosarcoma malignancy by regulating the Wnt/β-catenin pathway[6]. However, the function and mechanism of BAIAP2L2 in HCC development remain unclear. We further confirmed that BAIAP2L2 was significantly upregulated in HCC tissues and cell lines. BAIAP2L2 expression was closely related to HCC tumor size, vascular invasion, and tumor-node-metastasis (TNM) stage and was an independent risk factor for overall survival of HCC patients. In vitro and in vivo experiments showed that BAIAP2L2 promotes HCC cell proliferation, metastasis, stem cell activity, and cell cycle progression and inhibits apoptosis, suggesting that BAIAP2L2 plays an oncogenic role in HCC. We further investigated the regulators of BAIAP2L2 in HCC and found that NFκB1 activated the expression of BAIAP2L2 by binding to its promoter region.

Through database analysis, we found that GABPB1 was a downstream target of BAIAP2L2. GA-binding protein transcription factor subunit beta 1 (GABPB1), encoded by a single gene on chromosome 15q21, is a transcription factor that interacts with purine-rich repeats (GA repeats)[19]. GABPB1 is involved in the progression of various tumours[17,27]. Studies have shown that GABPB1 is a master regulator of nuclear-encoded mitochondrial genes, and GABPB1 overexpression in HCC promotes PRDX5 peroxidase gene expression, thus downregulating ROS levels[17]. Our results indicated that BAIAP2L2 could bind to GABPB1 through the Src homology 3 (SH3) domain. BAIAP2L2 inhibited the proteasomal degradation of GABPB1 by inhibiting its ubiquitination and promoted GABPB1 nuclear translocation. A series of rescue experiments showed that GABPB1 mediated the effects of BAIAP2L2 on promoting HCC progression.

The ETS family transcription factor GABPA and its partner GABPB1 activate the mutated telomerase reverse transcriptase (TERT) promoter in tumors. TRET promotes telomerase activation and is closely related to the malignancy of various tumors, and targeting TERT/telomerase is one direction of current cancer therapy[28]. Upregulation of TERT expression in tumor cells depends on its promoter mutation (− 124 and − 146 upstream of ATG, and both are C > T transitions)[29]. TERT promoter mutations occur in most hepatocellular carcinomas, bladder cancers and other malignancies[30,31]. Studies have shown that GABPA depletion or knockdown of GABPB1 to disrupt the GABPA/GABPB1 complex inhibits TERT expression. However, GABPA functions as a tumor suppressor, despite its stimulatory effect on TERT expression[32,33]. Hence, targeting GAPPB1 to regulate TRET is more valuable in the treatment of HCC. We found that BAIAP2L2 upregulated GABPB1 protein levels in HCC cells by inhibiting GABPB1 protein degradation and promoting its nuclear translocation. Therefore, we hypothesized that BAIAP2L2 can regulate TERT expression by promoting the formation of the GABPA/GABPB1 complex, thereby promoting the progression of HCC. Our data show that BAIAP2L2 expression is positively correlated with

TERT in HCC and that BAIAP2L2 promotes the mRNA and protein levels of TERT in HCC cells by regulating GABPB1. Collectively, BAIAP2L2 may be a new target for TERT/telomerase targeted therapy.

In conclusion, we identified the function and mechanism of BAIAP2L2 as an oncogene in HCC and, for the first time, revealed the function of the NFκB1/BAIAP2L2/GABPB1/TERT axis in HCC (Fig. 8G). Our study provides potential therapeutic targets and biomarkers for HCC.

Declarations

Funding

This work was supported by grants from the National Natural Science Foundation of China (81871260); Health Research Projects of Jiangsu Provincial Health Committee (H2019045); The training program of “Double hundred” young and middle-aged medical and health talents in Wuxi (BJ020034); Health Research Projects of Wuxi Health Committee(M202106); Key research and development Projects of Anhui Province (2022e07020048).

Declaration of competing interest

The authors declare that they have no known competing financial interests or personal relationships that could have appeared to influence the work reported in this paper.

Acknowledgments

Not applicable.

References

1. Torre, L. A. *et al.* Global cancer statistics, 2012. *CA: a cancer journal for clinicians* **65**, 87–108, doi:10.3322/caac.21262 (2015).
2. Siegel, R. L., Miller, K. D. & Jemal, A. Cancer statistics, 2015. *CA: a cancer journal for clinicians* **65**, 5–29, doi:10.3322/caac.21254 (2015).
3. Feng, R. M., Zong, Y. N., Cao, S. M. & Xu, R. H. Current cancer situation in China: good or bad news from the 2018 Global Cancer Statistics? *Cancer communications (London*, England) **39**, 22, doi:10.1186/s40880-019-0368-6 (2019).
4. Pinyol, R. *et al.* Molecular predictors of prevention of recurrence in HCC with sorafenib as adjuvant treatment and prognostic factors in the phase 3 STORM trial. Gut **68**, 1065–1075, doi:10.1136/gutjnl-2018-316408 (2019).
5. Xu, L. *et al.* BAI1–associated protein 2–like 2 is a potential biomarker in lung cancer. Oncology reports **41**, 1304–1312, doi:10.3892/or.2018.6883 (2019).
6. Guo, H. *et al.* BAIAP2L2 promotes the proliferation, migration and invasion of osteosarcoma associated with the Wnt/β-catenin pathway. Journal of bone oncology **31**, 100393,

doi:10.1016/j.jbo.2021.100393 (2021).

7. Liu, J., Shangguan, Y., Sun, J., Cong, W. & Xie, Y. BAIAP2L2 promotes the progression of gastric cancer via AKT/mTOR and Wnt3a/β-catenin signaling pathways. Biomedicine & pharmacotherapy = Biomedecine & pharmacotherapie **129**, 110414, doi:10.1016/j.biopha.2020.110414 (2020).
8. Liu, S., Wang, W., Zhao, Y., Liang, K. & Huang, Y. Identification of Potential Key Genes for Pathogenesis and Prognosis in Prostate Cancer by Integrated Analysis of Gene Expression Profiles and the Cancer Genome Atlas. Frontiers in oncology **10**, 809, doi:10.3389/fonc.2020.00809 (2020).
9. Hu, W., Wang, G., Yarmus, L. B. & Wan, Y. Combined Methylome and Transcriptome Analyses Reveals Potential Therapeutic Targets for EGFR Wild Type Lung Cancers with Low PD-L1 Expression. Cancers **12**, doi:10.3390/cancers12092496 (2020).
10. Livak, K. J. & Schmittgen, T. D. Analysis of relative gene expression data using real-time quantitative PCR and the 2(-Delta Delta C(T)) Method. Methods (San Diego, Calif.) **25**, 402–408, doi:10.1006/meth.2001.1262 (2001).
11. Broutier, L. *et al.* Human primary liver cancer-derived organoid cultures for disease modeling and drug screening. Nature medicine **23**, 1424–1435, doi:10.1038/nm.4438 (2017).
12. Zhu, P. *et al.* LncBRM initiates YAP1 signalling activation to drive self-renewal of liver cancer stem cells. Nature communications **7**, 13608, doi:10.1038/ncomms13608 (2016).
13. Nio, K., Yamashita, T. & Kaneko, S. The evolving concept of liver cancer stem cells. Molecular cancer **16**, 4, doi:10.1186/s12943-016-0572-9 (2017).
14. Hua, F. *et al.* TRIB3 Interacts With β-Catenin and TCF4 to Increase Stem Cell Features of Colorectal Cancer Stem Cells and Tumorigenesis. Gastroenterology **156**, 708–721.e715, doi:10.1053/j.gastro.2018.10.031 (2019).
15. Zheng, H. *et al.* Single-cell analysis reveals cancer stem cell heterogeneity in hepatocellular carcinoma. Hepatology (Baltimore, Md.) **68**, 127–140, doi:10.1002/hep.29778 (2018).
16. Tsuchiya, B., Sato, Y., Kameya, T., Okayasu, I. & Mukai, K. Differential expression of N-cadherin and E-cadherin in normal human tissues. Archives of histology and cytology **69**, 135–145, doi:10.1679/aohc.69.135 (2006).
17. Qi, W. *et al.* LncRNA GABPB1-AS1 and GABPB1 regulate oxidative stress during erastin-induced ferroptosis in HepG2 hepatocellular carcinoma cells. Scientific reports **9**, 16185, doi:10.1038/s41598-019-52837-8 (2019).
18. Yuan, X., Dai, M. & Xu, D. TERT promoter mutations and GABP transcription factors in carcinogenesis: More foes than friends. Cancer letters **493**, 1–9, doi:10.1016/j.canlet.2020.07.003 (2020).
19. Mancini, A. *et al.* Disruption of the β1L Isoform of GABP Reverses Glioblastoma Replicative Immortality in a TERT Promoter Mutation-Dependent Manner. Cancer cell **34**, 513–528.e518, doi:10.1016/j.ccell.2018.08.003 (2018).
20. Shay, J. W. & Wright, W. E. Telomeres and telomerase: three decades of progress. Nature reviews. Genetics **20**, 299–309, doi:10.1038/s41576-019-0099-1 (2019).

21. Yuan, X., Dai, M. & Xu, D. Telomere-related Markers for Cancer. Current topics in medicinal chemistry **20**, 410–432, doi:10.2174/1568026620666200106145340 (2020).
22. Yuan, X., Larsson, C. & Xu, D. Mechanisms underlying the activation of TERT transcription and telomerase activity in human cancer: old actors and new players. Oncogene **38**, 6172–6183, doi:10.1038/s41388-019-0872-9 (2019).
23. Pykäläinen, A. *et al.* Pinkbar is an epithelial-specific BAR domain protein that generates planar membrane structures. Nature structural & molecular biology **18**, 902–907, doi:10.1038/nsmb.2079 (2011).
24. Chen, Z., Shi, Z. & Baumgart, T. Regulation of membrane-shape transitions induced by I-BAR domains. Biophysical journal **109**, 298–307, doi:10.1016/j.bpj.2015.06.010 (2015).
25. Millard, T. H. *et al.* Structural basis of filopodia formation induced by the IRSp53/MIM homology domain of human IRSp53. The EMBO journal **24**, 240–250, doi:10.1038/sj.emboj.7600535 (2005).
26. Song, Y., Zhuang, G., Li, J. & Zhang, M. BAIAP2L2 facilitates the malignancy of prostate cancer (PCa) via VEGF and apoptosis signaling pathways. Genes & genomics **43**, 421–432, doi:10.1007/s13258-021-01061-8 (2021).
27. Chen, S. C. *et al.* Knockdown of GA-binding protein subunit β1 inhibits cell proliferation via p21 induction in renal cell carcinoma. International journal of oncology **53**, 886–894, doi:10.3892/ijo.2018.4411 (2018).
28. Chen, X., Tang, W. J., Shi, J. B., Liu, M. M. & Liu, X. H. Therapeutic strategies for targeting telomerase in cancer. Medicinal research reviews **40**, 532–585, doi:10.1002/med.21626 (2020).
29. Huang, F. W. *et al.* Highly recurrent TERT promoter mutations in human melanoma. Science (New York, N.Y.) **339**, 957–959, doi:10.1126/science.1229259 (2013).
30. Nault, J. C. *et al.* Telomerase reverse transcriptase promoter mutation is an early somatic genetic alteration in the transformation of premalignant nodules in hepatocellular carcinoma on cirrhosis. Hepatology (Baltimore, Md.) **60**, 1983–1992, doi:10.1002/hep.27372 (2014).
31. Guo, Y. *et al.* GABPA is a master regulator of luminal identity and restrains aggressive diseases in bladder cancer. Cell death and differentiation **27**, 1862–1877, doi:10.1038/s41418-019-0466-7 (2020). **Legend**

Tables

Table 1 Correlation between BAIAP2L2 expression and clinicopathological features.

Clinicopathological features	All cases		BAIAP2L2		*p* value
			High expression	Low expression	
Age (years)	>60	52	28	24	
	≤60	28	12	16	0.3484
Gender	Female	37	17	20	
	Male	43	23	20	0.5011
HBV	Negative	19	8	11	
	Positive	61	32	29	0.4306
Tumor multiplicity	Single	54	22	32	
	Multiple	26	18	8	**0.0170***
Tumor size (cm)	≤5	47	19	28	
	>5	33	21	12	**0.0410***
α-fetoprotein (ng/ml)	≤200	35	17	18	
	>200	45	23	22	0.8217
Edmondson stage	I-II	49	19	30	
	III-IV	31	21	10	**0.0018****
TNM stage	I	37	14	23	
	II-III	43	26	17	**0.0436***
Microvascular invasion	Yes	37	25	12	
	No	43	15	28	**0.0036****

*p < 0.05, **P < 0.01.

Table 2 Univariate and multivariate analysis of factors associated with overall survival of 80 HCC patients

Clinicopathologic Parameters	Univariable analysis			Multivariable analysis		
	HR	95%CI	P value	HR	95%CI	P value
Age (>50 years vs ≤ 50 years)	0.49	0.23-1.1	0.074			
Gender (female vs male)	1.3	0.7-2.4	0.43			
HBV infection (positive vs negative)	0.8	0.39-1.6	0.55			
TNM stage (II/III vs I)	1.3	0.71-2.4	0.4			
Microvascular invasion (yes vs no)	1.9	1-3.4	**0.043***	1.306	0.683-2.495	0.419
Tumor multiplicity (multiple vs simple)	1.8	0.91-3.1	**0.044***	1.34	0.704-2.548	0.373
α-fetoprotein (≥20 ng/ml vs < 20 ng/ml)	0.7	0.37-1.3	0.26			
Edmonson stage (III/IV vs I/II)	1.1	0.63-2.1	0.65			
Tumor size (≥5 cm vs < 5 cm)	2.4	1.3-4.5	**0.0065****	1.626	0.827-3.194	0.159
BAIAP2L2 expression (high vs low)	3.6	1.8-7.1	**<0.001*****	2.488	1.13-5.477	**0.024***

*p < 0.05, **p < 0.01, ***p < 0.001.

HR, hazard ratio; CI, confidence interval.

Figures

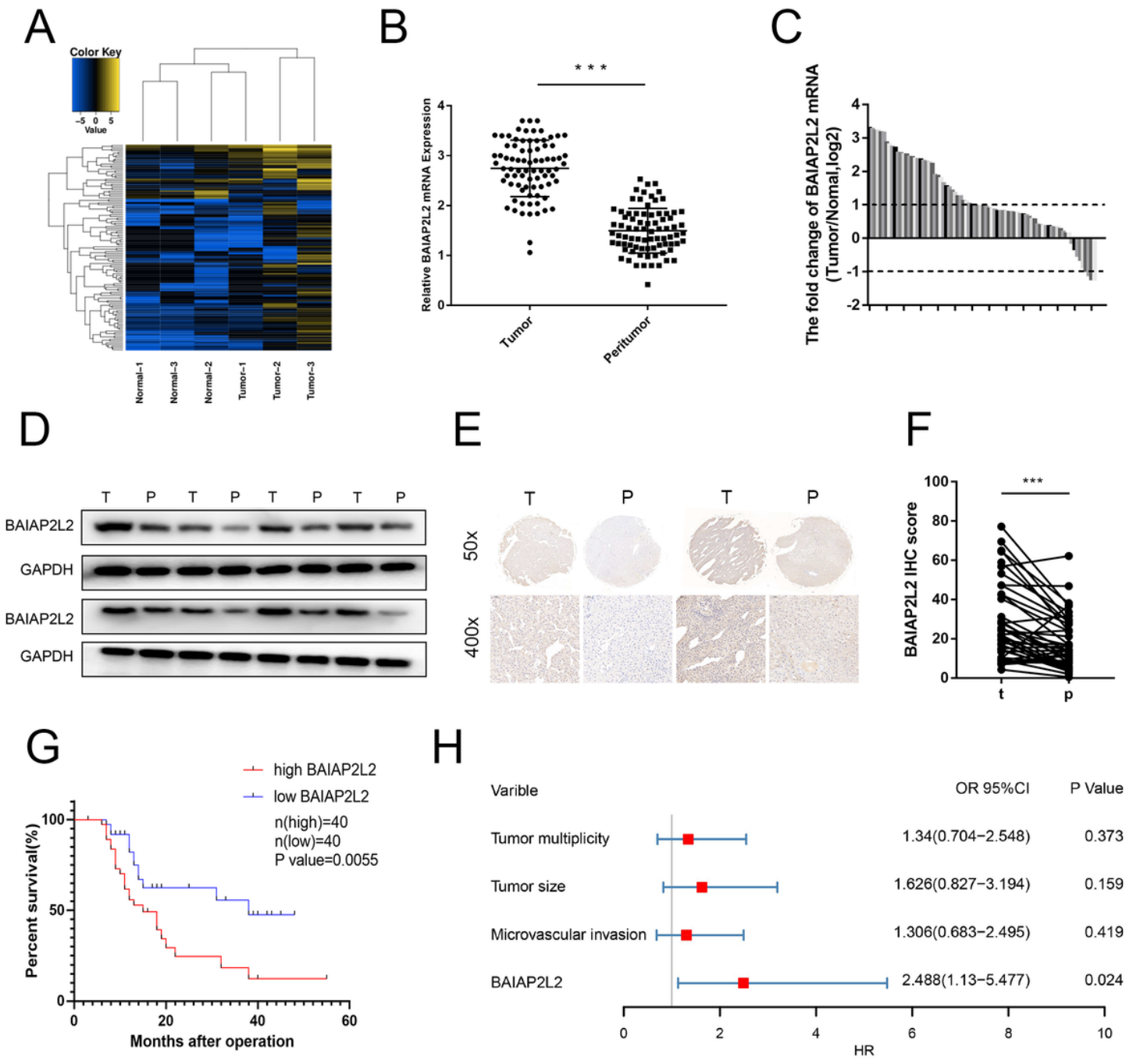

Figure 1

BAIAP2L2 expression is upregulated in HCC and associated with poor prognosis. A. Hierarchical clustering analysis of differentially expressed mRNAs between HCC tissues and adjacent noncancerous liver tissues (BAIAP2L2: 11.83-fold; p <0.001). B. qRT—PCR detection of BAIAP2L2 mRNA expression in 80 pairs of HCC specimens. C. The fold change in BAIAP2L2 mRNA expression between HCC and corresponding adjacent tissues. D. Western blot detection of BAIAP2L2 protein expression in 8 pairs of HCC tissues (T) and corresponding adjacent tissues (P). E. Immunohistochemical staining of BAIAP2L2 in 2 pairs of HCC tissues cut from 40 pairs of HCC tissue chips. The original magnifications were 50× and

400×. F. The quantification results of the BAIAP2L2 IHC score in 40 pairs of HCC tissues (t: Tumor, p: Peritumor). G. Overall survival analysis assessed the effect of BAIAP2L2 on overall survival in HCC. H. Multivariate analysis of hazard ratios for overall survival. *P< 0.05, **P< 0.01, ***P< 0.001.

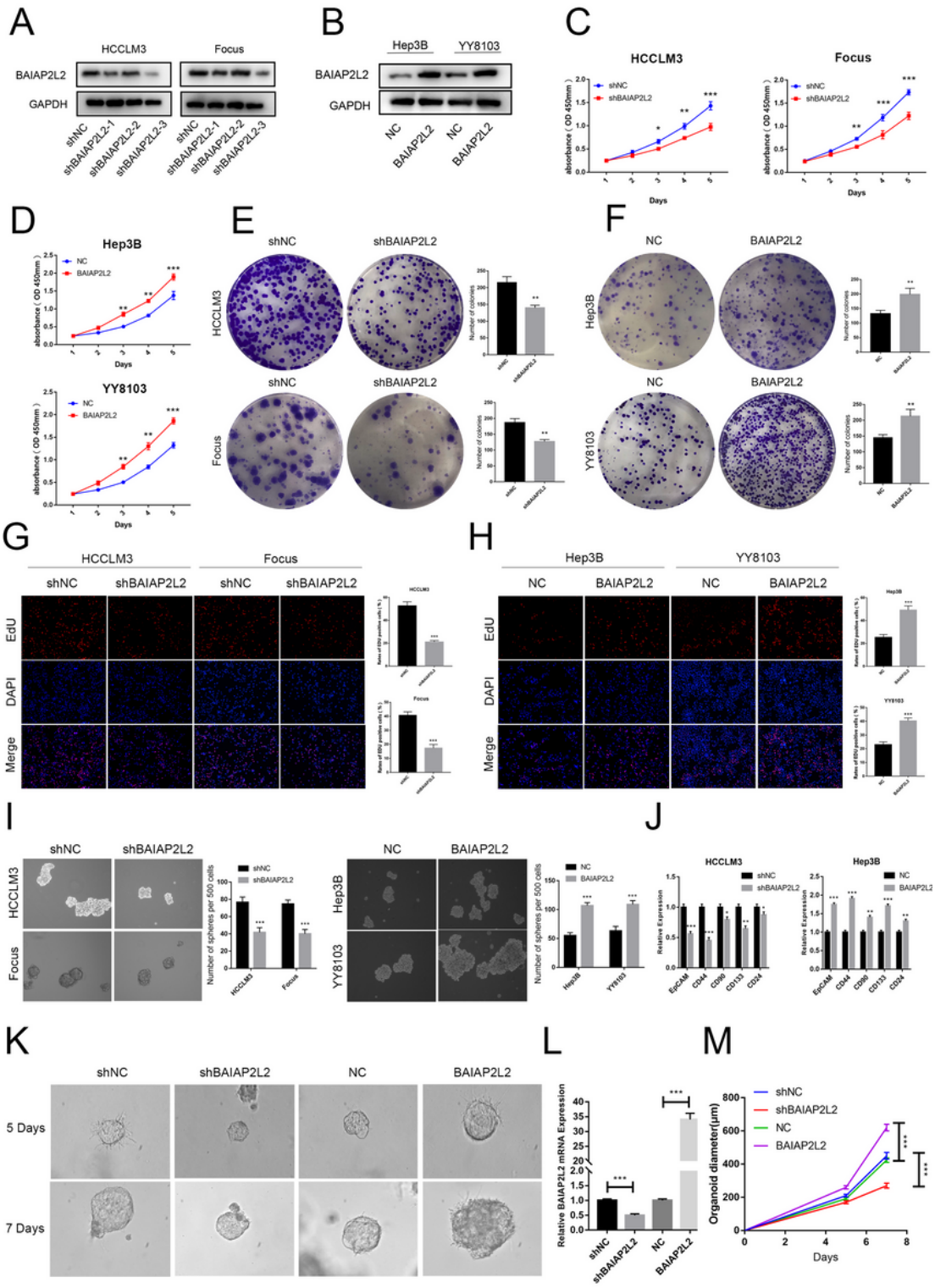

Figure 2

BAIAP2L2 promotes HCC cell proliferation and stem cell activity. A. Western blot detection of BAIAP2L2 knockdown efficiency after transfection of lentivirus-based small hairpin RNA (shRNA). B. After transfection with overexpressed BAIAP2L2 lentivirus, the expression level of BAIAP2L2 was detected by western blot. C-D. Growth curves based on the CCK-8 assay of BAIAP2L2-downregulated and BAIAP2L2-overexpressing HCC cells. E-F. The effect of BAIAP2L2 knockdown and overexpression on cell proliferation was detected by a colony formation assay. G-H. EdU assay was performed to detect the proliferation of HCC cells transfected with different lentiviruses. I. A stem cell spheroidization assay was conducted to detect the activity of HCC stem cells with BAIAP2L2 knockdown or overexpression. J. The expression of CSC-related genes in BAIAP2L2-knockdown and BAIAP2L2-overexpressing HCC hepatospheres was examined by qRT—PCR. K. Images of HCC organoids infected with BAIAP2L2-knockdown or -overexpression lentivirus. L. BAIAP2L2 expression levels in organoids were measured by qRT—PCR. M. Growth curves of HCC organoids after lentiviral infection. *P< 0.05, **P< 0.01, ***P< 0.001.

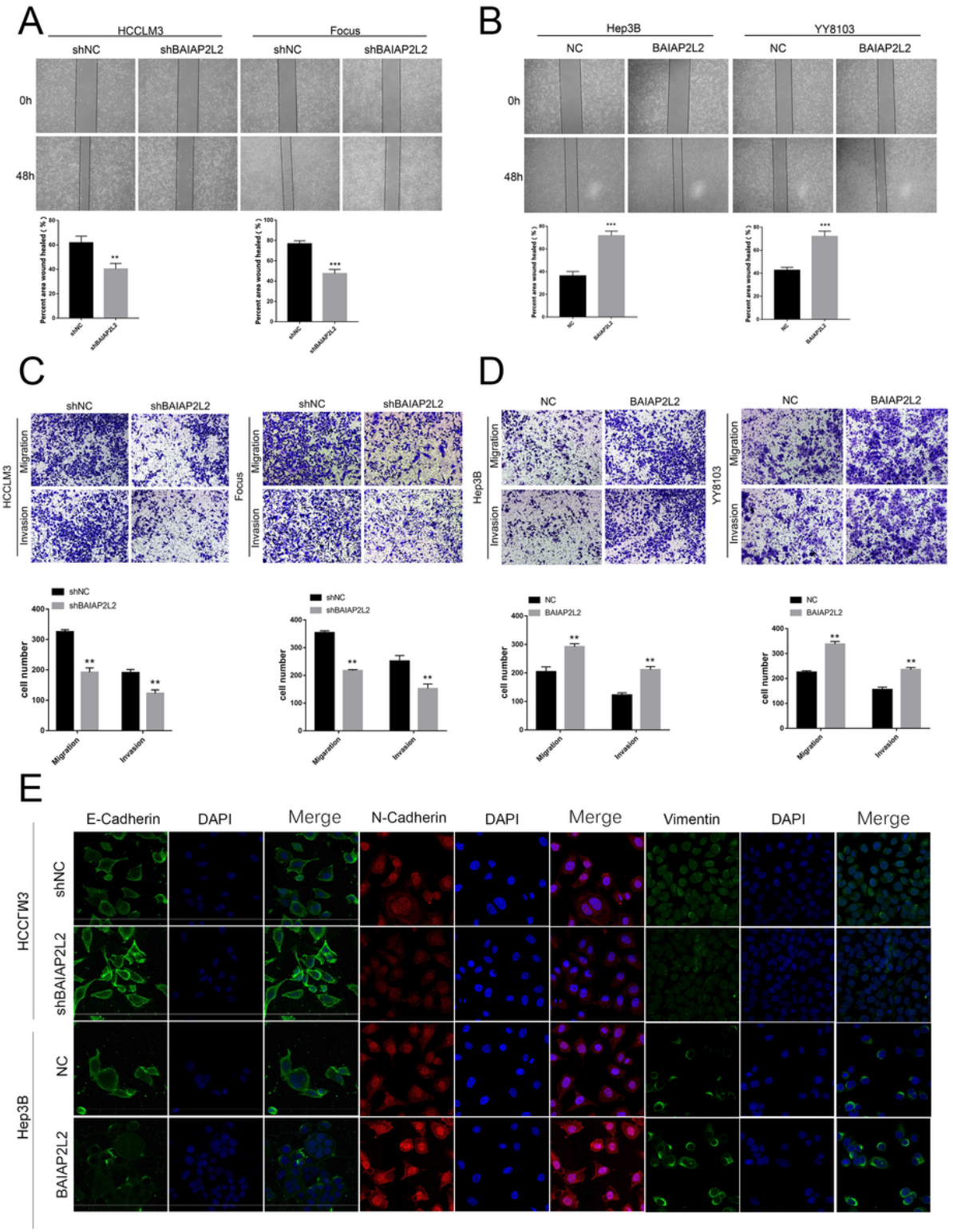

Figure 3

BAIAP2L2 promotes cell migration and invasion and activates the EMT pathway in HCC. A-B. The role of BAIAP2L2 in the regulation of cell motility was assessed by wound-healing experiments. C-D. Transwell assays were performed to detect the effect of BAIAP2L2 downregulation and overexpression on cell migration and invasion. E. The expression of EMT-related proteins was detected by immunofluorescence in HCCLM3 and Hep3B cells. *P< 0.05, **P< 0.01, ***P< 0.001.

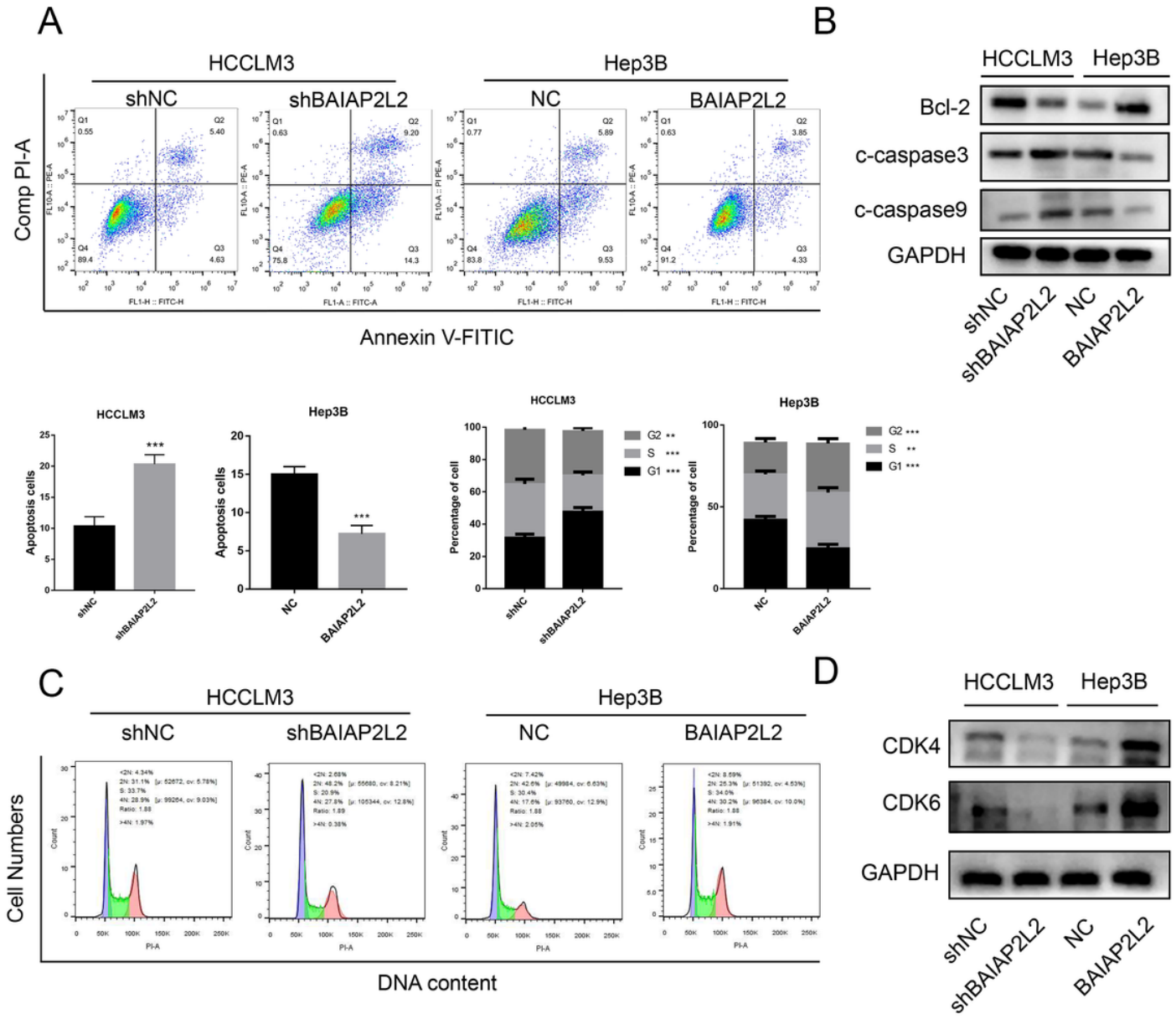

Figure 4

BAIAP2L2 inhibits apoptosis and accelerates the G1/S cell cycle in vitro. A. The role of BAIAP2L2 in the regulation of HCC cell apoptosis was verified by flow cytometry. B. Western blotting was used to detect apoptosis-related proteins in HCC cells after BAIAP2L2 knockdown or overexpression. C. The cell cycle results of HCC cells with BAIAP2L2 overexpression or knockdown. D. The expression of cell cycle-related proteins was examined by western blot. *P< 0.05, **P< 0.01, ***P< 0.001.

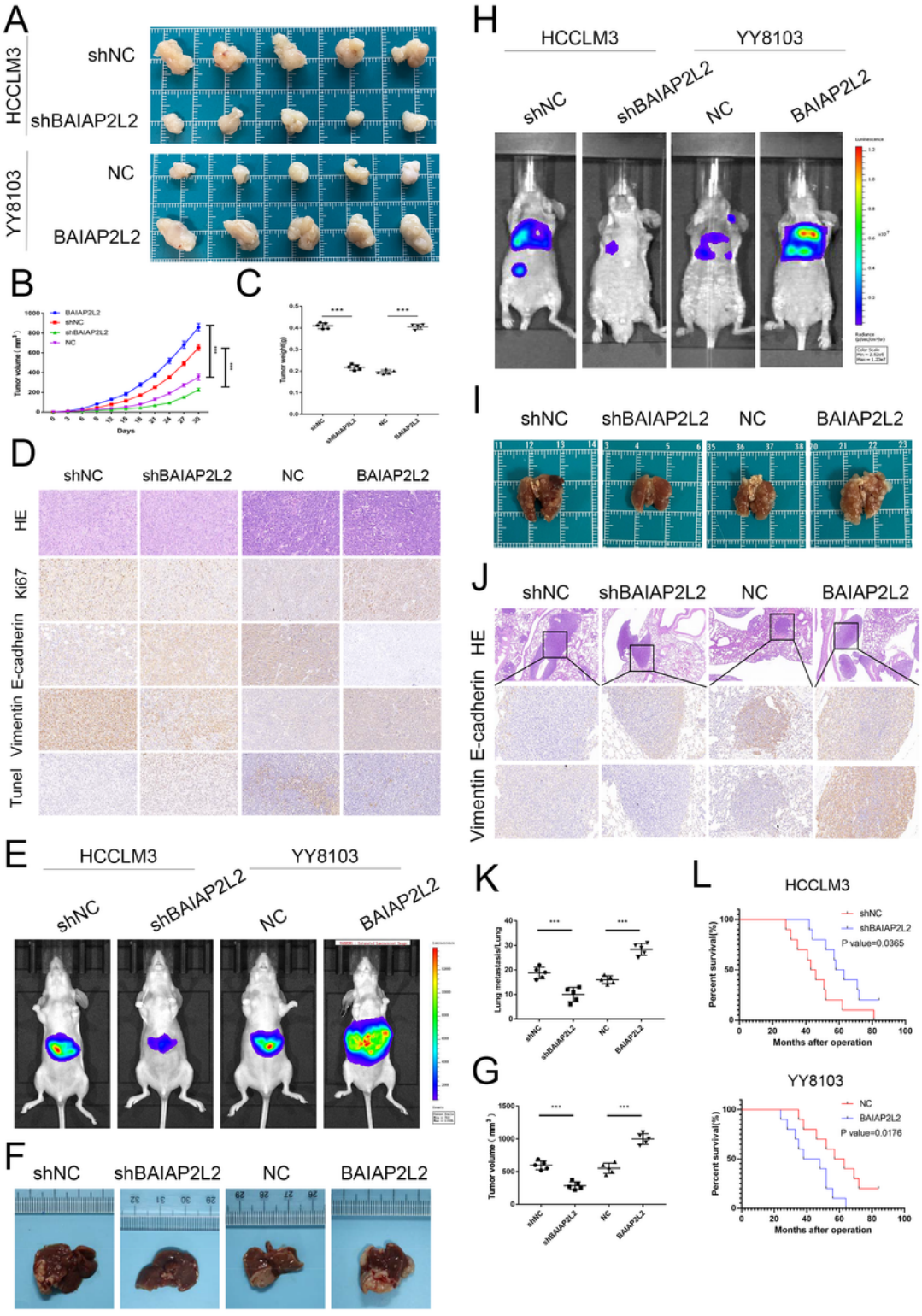

Figure 5

BAIAP2L2 potentiates HCC growth and metastasis in vivo. A. Photograph of tumors obtained from nude mice. B-C. Tumor weight and growth curves of the volumes of the xenografts. D. Representative pictures of the protein levels of Ki67 and E-cadherin. Vimentin and TUNEL were detected by immunohistochemistry in four groups of subcutaneous tumor tissues. Original magnification 400 ×. E. Fluorescence intensity was measured in nude mouse livers orthotopically implanted with treated

HCCLM3 and YY8103 cells. F. Images of the orthotopic tumor transplantation model. G. Volumes of the xenograft-implanted tumors. H. Bioluminescence photographs of the metastasis model in nude mice with tail vein injection of BAIAP2L2 knockdown HCCLM3 cells and BAIAP2L2 overexpression YY8108 cells. I. Representative images of lung tissues of the indicated four groups. J. HE staining and immunohistochemical detection of E-cadherin and vimentin of pulmonary metastases. Original magnification 100× and 400×. K. The number of lung metastatic foci was counted. L. Overall survival curve of mice in the four groups. *P< 0.05, **P< 0.01, ***P< 0.001.

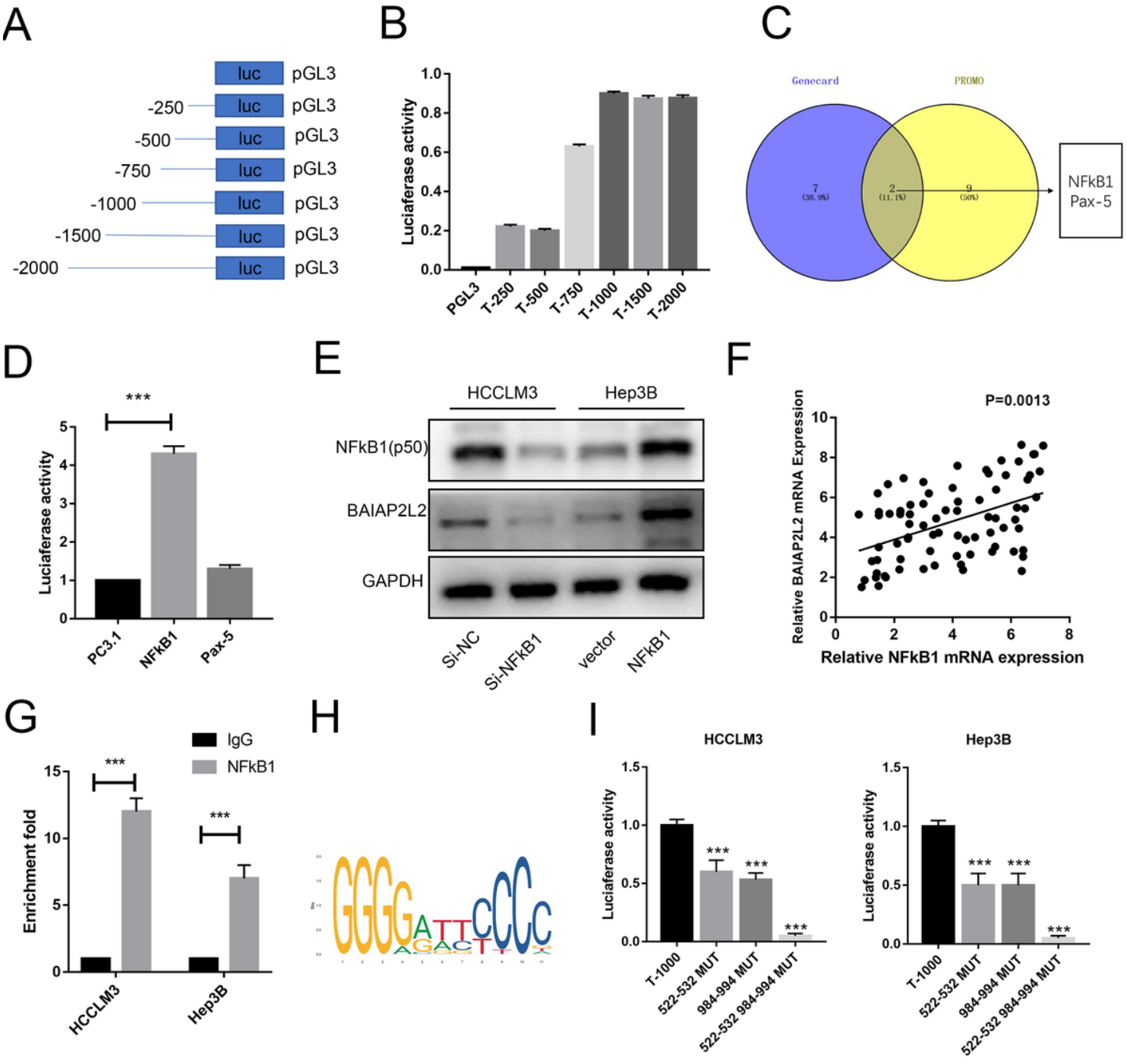

Figure 6

NFκB1 activates BAIAP2L2 transcription in HCC cells. A. Schematic diagram of the BAIAP2L2 promoter fragments of -2000~0 bp, -1500~0 bp, -1000~0 bp, -750~0 bp, -500~0 bp and -250~0 bp cloned upstream of the firefly luciferase reporter gene in the pGL3-basic vector. B. Detection of the transcriptional activity of the BAIAP2L2 promoter fragment by luciferase activity assays in 293T cells. C. Venn diagram showing that NFκB1 and Pax-5 were predicted to bind to the BAIAP2L2 promoter by Genecard and PROMO. D. Luciferase activity assays demonstrated that NFκB1 observably increases the promoter activities of pGL3−1000/0. E. Western blot assays showed that knockdown of NFκB1 inhibits the expression of BAIAP2L2 in HCCLM3 cells and that overexpression of NFκB1 enhances the expression of BAIAP2L2 in Hep3B cells. F. Spearman's correlation analysis was performed to analyze the association between NFκB1 and BAIAP2L2 in 80 HCC samples. G. ChIP—qPCR analysis showed that the BAIAP2L2 promoter fragment could be enriched by an anti-NFκB1 antibody in HCCLM3 and Hep3B cells. H. The binding motif of NFκB1 was obtained from the JASPAR database. I. Luciferase activity of the BAIAP2L2 promoter was reduced when (−522 to −532 bp), (−984 to −994 bp) and the two-site mutation (−522 to −532 bp, −984 to −994 bp) were mutated in HCCLM3 and Hep3B cells. *P< 0.05, **P< 0.01, ***P< 0.001.

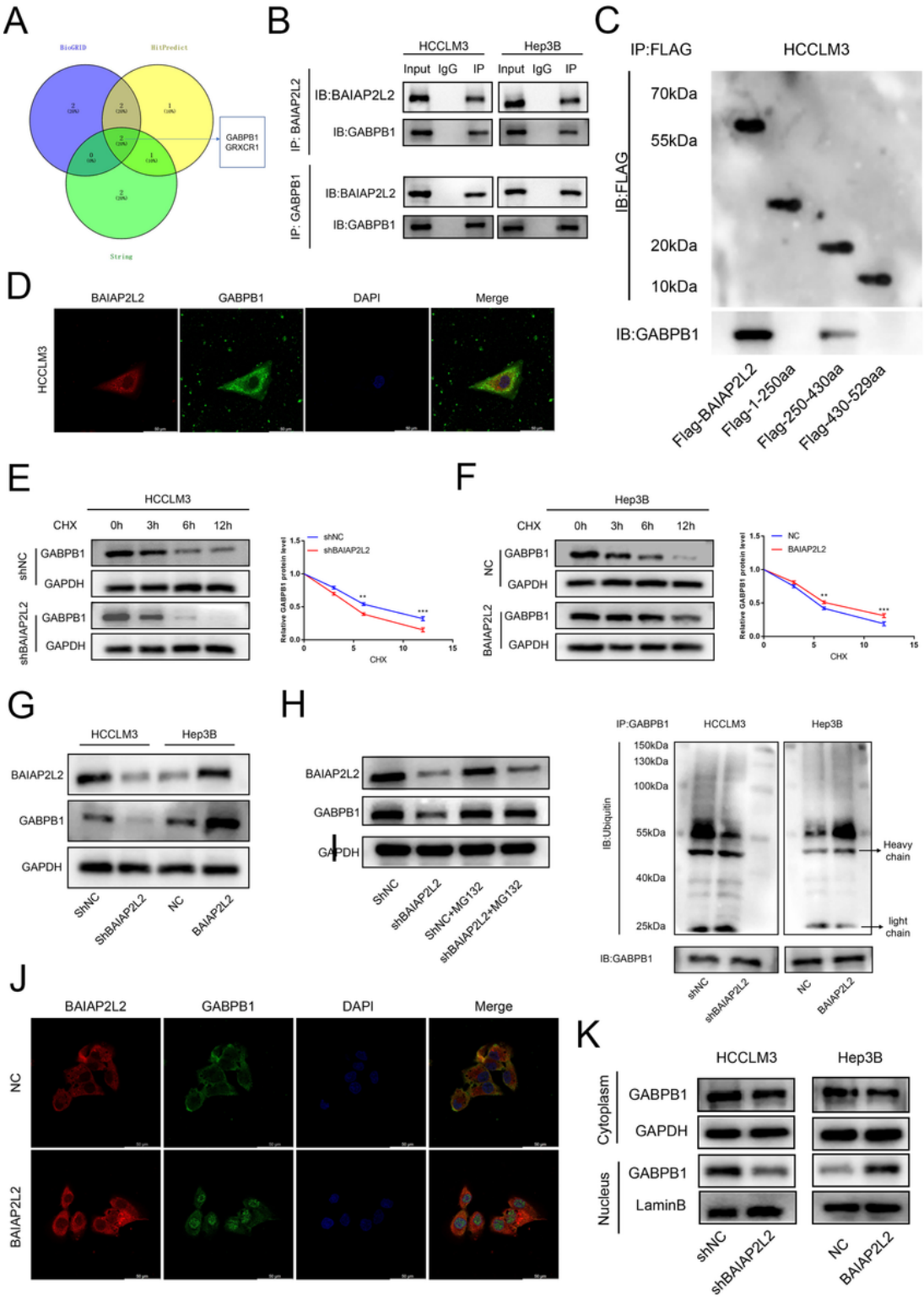

Figure 7

BAIAP2L2 inhibited the ubiquitin-mediated degradation of GABPB1 and promoted GABPB1 nuclear translocation. A. The BAIAP2L2-interacting proteins were predicted using the BioGRID, STRING and HitPredict databases. B. Co-IP experiments showed that GABPB1 could be enriched by anti-BAIAP2L2 antibody, and BAIAP2L2 was immunoprecipitated with anti-GABPB1 antibody. C. Co-IP assay was performed to examine the relationship between GABPB1 and full-length BAIAP2L2 or truncated BAIAP2L2

in HCCLM3 cells. D. Immunofluorescence assay showed that BAIAP2L2 and GABPB1 co-localized in HCCLM3 cells. Scale bar, 50 μm. E-F. Western blot analysis detected GABPB1 expression changes in BAIAP2L2 knockdown or overexpression HCC cells after cycloheximide (CHX) treatment. The relative GABPB1 protein level was graphed. G. GABPB1 expression in HCC cells with BAIAP2L2 knockdown or overexpression was examined by western blot. H. Western blot analysis showed that the expression level of GABPB1 was restored in HCCLM3-shBAIAP2L2 cells after MG132 treatment. I. Co-IP assay to detect the effect of BAIAP2L2 expression on GABPB1 ubiquitination. J. Immunofluorescence staining of BAIAP2L2 and GABPB1 in BAIAP2L2-overexpressing Hep3B cells and NC-Hep3B cells. K. Expression of GABPB1 in the cytoplasm and nucleus of BAIAP2L2-overexpressing Hep3B cells or BAIAP2L2-knockdown HCCLM3 cells was analyzed by western blot. *P< 0.05, **P< 0.01, ***P< 0.001.

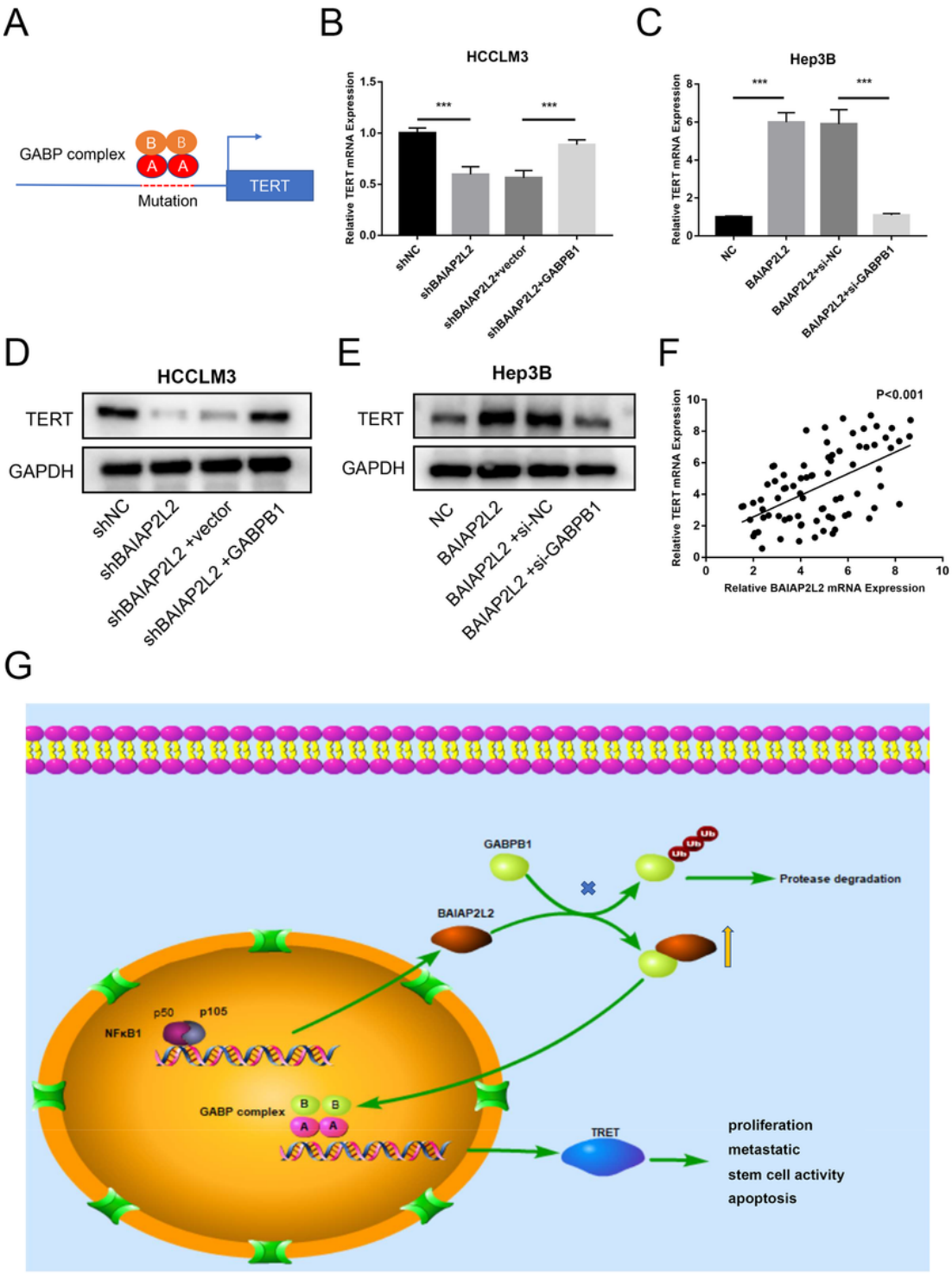

Figure 8

BAIAP2L2 regulates TERT by upregulating GABPB1. A. The GABPA-GABPB1 complex could bind and activate the mutant TERT promoter. B-C. qRT-PCR analysis showed that TERT mRNA expression in HCCLM3-shBAIAP2L2 was decreased and GABPB1 overexpression was restored, the opposite results were obtained in Hep3B cells with BAIAP2L2 overexpression and GABPB1 knockdown. D-E. Western blot further verified the expression of TERT protein in treated HCCLM3 and Hep3B cells. F. Spearman's

correlation analysis was performed to determine the association between BAIAP2L2 and TERT in 60 HCC samples. G. Integrated model describing the mechanism of the oncogenic role of BAIAP2L2 in HCC. The model shows that BAIAP2L2 is translationally regulated by NFκB1. BAIAP2L2 interacts with GABPB1 to inhibit its ubiquitin-mediated degradation and promote its nuclear translocation, thereby upregulating the expression of TERT. *P< 0.05, **P< 0.01, ***P< 0.001.

Supplementary Files

This is a list of supplementary files associated with this preprint. Click to download.

- Fig.s1.tif
- Fig.s2.tif
- Fig.s3.tif
- Fig.s4.tif
- Fig.s5.tif
- Supplementarytable1.xlsx
- supporttable.docx
- SupportFigureLegend.docx
- Westernblotrawmaterial.pdf